Biochimica et Biophysica Acta, 1112 (1992) 197–204

BBAMEM 75825

Shear stress-facilitated calcium ion transport across lipid bilayers

Srinivasa R. Chakravarthy [1] and Todd D. Giorgio

Department of Chemical Engineering, Vanderbilt University, Nashville, TN (USA)

(Received 25 May 1992)
(Revised manuscript received 24 August 1992)

Key words: Liposome; Fluid force; Calcium permeability; Shear stress; Fluorescence; Ion transport

Small unilamellar liposomes were used in this study of shear stress effects on the trans-bilayer flux of calcium ions (Ca^{2+}). Liposome suspensions were prepared from 99% egg phosphatidylcholine by a microporous filter extrusion technique. The inner aqueous phase of the unilamellar liposomes contained indo-1^{5-}, a fluorescent indicator of free Ca^{2+}. The external aqueous phase was composed of Hepes-buffered saline containing normal physiological levels of common ionic species. Calcium ion levels were set at 100 nM and 1 mM in the inner and outer aqueous phases, respectively. Liposome suspensions were exposed to graded levels of uniform shear stress in an optically modified rotational viscometer. Intraliposome Ca^{2+} concentration was estimated from continuous measurement of indo-1^{5-} fluorescence. Electronically measured particle size distribution was used to determine liposome surface area for estimation of trans-bilayer Ca^{2+} flux. Trans-bilayer Ca^{2+} flux increased linearly with applied shear rate from 27 s^{-1} to 2700 s^{-1}. Diffusional resistance of the lipid bilayer, not the convective resistance of the surrounding fluid, was the limiting step in the transport of Ca^{2+}. Liposome permeability to Ca^{2+} increased by nearly two orders of magnitude over the physiologically relevant shear rate range studied. Solute transport in injectable liposome preparations may be dramatically influenced by cardiovascular fluid stress. Solute delivery rates determined in liposomes exposed to static conditions may not accurately predict in vivo, cardiovascular solute transport.

Introduction

Injectable liposomes experience a well recognized, but less well understood, hostile environment in terms of cellular and biological hazards. Spatially or temporally controlled release of solute(s) from the liposome encapsulated volume is frequently an important consideration in their application. The influence of thermal and chemical cardiovascular conditions on liposome permeability have been studied for a wide variety of systems in an effort to improve in vivo performance [1–4].

Passive transport of small solutes and ions across liposome membranes occurs primarily at the site of local, transient defects in membrane structure [5–7]. These defects may result from the incorporation of small hydrophobic solutes which disrupt ordered lipid packing [8], from thermal fluctuations near the lipid liquid-gel phase transition [6] and at the site of lipid/protein interfaces [7]. Lipid monolayers studied by X-ray diffraction and observed directly by fluorescence microscopy possess such packing defects [9].

Lipid bilayer permeability can also be influenced by the application of physical stress, such as occurs in electro-mechanical permeabilization [10] or isothermal exposure to microwave radiation [11]. Application of lateral pressure (F_{LP}) to lipid bilayers modifies the area occupied by each lipid molecule. The relationship between F_{LP} and molecular area (A_M) is the bilayer compressibility [12]. Bilayer compressibility is a function of bilayer composition, lipid properties (hydrocarbon tail structure and headgroup charge and size) and temperature. Compressibility has been related to the rate of trans-bilayer solute transport [13]. Enhanced permeability has been predicted for lipid bilayers with high compressibility [14].

The modest fluid forces developed in the mammalian cardiovascular system are generally not sufficient to modify liposomes in a macroscopic way. The influence of fluid shear stress on bilayer permeability and subsequent in vivo liposome performance is unknown. Convective mass transfer also influences solute transport in liposomes exposed to bulk fluid motion.

The rate of solute delivery from liposome suspensions is usually determined in either a stagnant container or in a mixed vessel with unknown and unquan-

Correspondence to: T.D. Giorgio, Vanderbilt University, Box 60, Station B Nashville, TN 37235, USA.
[1] Present address: Trinity Consultants, Inc., 9401 Indian Creek Parkway, Suite 970, Overland Park, KS 66210, USA.

tified fluid forces. Delivery rates determined under static or undefined conditions may not accurately predict solute transport from liposomes exposed to in vivo cardiovascular fluid stress. This work seeks to experimentally determine the rate of Ca^{2+} transport across a lipid bilayer as a function of fluid shear stress. Transbilayer Ca^{2+} flux was determined as a function of the uniform, controlled shear stress applied to the liposome sample in a cone and plate rotational viscometer. The intraliposome free calcium ion concentration ($[Ca^{2+}]_i$) was estimated from the fluorescence response of the Ca^{2+}-sensitive indicator indo-1^{5-}. A similar optical technique has been used to study Ca^{2+} [15,16], K^+ [17] and Cl^- [18] transport across liposome bilayers in the absence of fluid stress. Extension of these studies may help elucidate the potential role of membrane permeability changes in shear stress induced cellular activation.

Materials and Methods

Materials. Egg phosphatidylcholine (99% pure), chloroform, ethylenediaminetetraacetic acid (EDTA), *N*-(2-hydroxyethyl)piperazine-*N'*-2-ethanesulfonic acid (Hepes), $MgCl_2$, $CaCl_2$, KCl, Na_2HPO_4, NaCl, NaN_3 were purchased from Sigma. Sepharose CL-4B and the gel filtration column apparatus were purchased from Pharmacia. The extruder used in liposome preparation was purchased from Lipex Biomembranes. The polycarbonate membrane filters were obtained from Poretics. The electronic particle counter (model Elzone 280 PC) used for counting and sizing the liposomes was purchased from Particle Data. Indo-1^{5-}, a fluorescent indicator of free Ca^{2+} concentration, was obtained from Molecular Probes. The cone and plate viscometer used in this study was a Weissenberg Rheogoniometer, model R.18. The cone was nominally 1° with a diameter of 10 cm. The fiber optic bundles, xenon arc source and interference filters were purchased from Oriel. The xenon arc power supply was produced by Photon Technology International; the photomultiplier tube housings and photomultiplier tube power supplies from Pacific Instruments. Photomultiplier tube amplifiers were purchased from United Detector Technology. Digital data acquisition was performed with analog/digital conversion hardware (model DASH-16, MetraByte) fitted in a microcomputer (model 286-16, CompuAdd) under software control (Labtech Notebook).

Liposome sample preparation. 200 mg of 99% egg phosphatidylcholine were dissolved in 2 ml of chloroform and placed in a flask attached to a rotary vacuum evaporator (RVE). The dissolved lipid solution was evaporated under vacuum (10 inch Hg) at 40°C and 2 RPM until no trace of the solvent remained. The thin lipid film produced was hydrated in Ca^{2+}-free Hepes buffered saline at a pH of 7.4, containing indo-1^{5-} (1 mM). Lipid concentration of the hydrated solution was 100 mg/ml of aqueous phase. This suspension was then rotated on the RVE at 40°C until complete hydration of the lipid film occurred. The multilamellar vesicle (MLV) suspension produced was equilibrated at room temperature for 3 h.

The pre-cleaned extrusion apparatus was fitted with two microporous filters stacked in series and rinsed with Ca^{2+}-free Hepes buffered saline solution. The MLV suspension was introduced into the sample chamber and extruded through the membrane filters with nitrogen gas at a controlled temperature of 30°C. The nitrogen pressure was adjusted with a compressed gas regulator to maintain a liposome suspension flow rate of approx. 1 ml/min. The extrusion process was repeated 10 times to obtain well characterized, uniform unilamellar vesicles (ULV) [19,20]. The filter pore diameter was 1.0 μm for the first five extrusions and 0.8 μm for the final five extrusions.

Unencapsulated indo-1^{5-} was removed from the ULV suspension by gel filtration chromatography. ULV suspensions were layered on a Sepharose CL-4B column (2 cm diameter × 35 cm long) and eluted with Ca^{2+}-free Hepes buffer (pH 7.4) at a flow rate 0.75 ml/min. Absorbance (340 nm) of the eluent was monitored and fractions were collected manually. ULVs elute in the void volume with a retention time much shorter than that of the unencapsulated indo-1^{5-}; a clean separation was accomplished.

A 3.33 μl sample of the gel filtered ULV suspension was diluted with 20 ml of normal saline for electronic particle counting and sizing. Typical mode ULV diameter was 0.78 μm. The particle size distribution was used to calculate the volume fraction of ULVs in the gel filtered preparation. Final ULV concentration was adjusted to 0.3% by volume by dilution with Ca^{2+}-free Hepes buffer at pH 7.4. Total liposome surface area was determined from the particle size distribution of the diluted ULV preparation.

Calcium efflux measurement. Studies of Ca^{2+} flux across liposomes during shear stress exposure were done in an optically modified cone and plate viscometer. An aliquot of the ULV suspension was contained between the cone and plate of the viscometer. The common end of a bifurcated quartz fiber optic bundle is mounted flush with the surface of the stationary, upper flat viscometer platen. Fluorescence excitation illumination is delivered to the sample through one leg of the fiber optic bundle by a 75 watt xenon arc lamp bandpass filtered at 340 nm. Sample fluorescence collected at the common end of the fiber optic bundle is divided by optical connection to the common end of a second bifurcated fiber bundle. Each leg of the second bifurcation directs the fluorescence signal to an independent photomultiplier tube (PMT) detector. The flu-

orescent signal is filtered in the PMT housings by narrow bandpass filters centered at 410 nm and 490 nm. The microamp (μA) signal produced by the PMTs is amplified and measured as millivolts (mV) by analog-to-digital data acquisition hardware installed in a microcomputer.

Cone rotation was preset to the desired speed (0, 4, 225 or 450 revs./min, resulting in shear rates of 0, 27, 1350, 2700 s^{-1}, respectively). A fluorescence measurement was performed before shear exposure or addition of Ca^{2+} to the sample. A concentrated $CaCl_2$ solution was added to the exterior aqueous space to obtain a final concentration of 1 mM Ca^{2+}. Fluorescence measurements were recorded until Ca^{2+} saturation of the encapsulated indo-1^{5-} occurred. The sample was recovered from the viscometer at the conclusion of the experiment for calibration of the indo-1^{5-} fluorescence. The recovered ULV sample was sonicated for 30 s in an ultrasonic homogenizer and returned to the optically modified viscometer for measurement of the maximum fluorescence ratio (R_{max}). The minimum fluorescence ratio (R_{min}) was obtained by adding a final concentration of 2 mM EDTA to the sonicated sample. All additions were carried out in Hepes-buffered saline at pH 7.4. The minimum and the maximum fluorescence ratios are required in the calculation of free calcium ion concentration by the method of Grynkiewicz [21]:

$$[Ca^{2+}]_i = K_d \cdot \left[\frac{(R - R_{min})}{(R_{max} - R)}\right]$$

where K_d is the dissociation constant (250 nM) and R is the fluorescence ratio ($I_{410\ nm}/I_{490\ nm}$). $[Ca^{2+}]_i$ was estimated as a function of time. The $[Ca^{2+}]_i$ flux across the liposomes was then obtained from the unsteady Ca^{2+} balance:

$$\text{transmembrane } Ca^{2+} \text{ flux} = \left(\frac{V}{SA}\right) \cdot \frac{d[Ca^{2+}]_i}{dt}$$

where V is the total liposome encapsulated volume (cm^3), SA is the total liposome surface area (cm^2) and $d[Ca^{2+}]_i/dt$ is the time rate of change of $[Ca^{2+}]_i$ (determined as the slope of $[Ca^{2+}]_i$ vs. time). The volume and surface area of the ULV sample were obtained directly from the particle counter.

Results

Calcium transport across liposome membranes in the absence of fluid shear

Fig. 1 shows a typical measurement of intraliposomal free calcium ion concentration ($[Ca^{2+}]_i$) as a function of time after Ca^{2+} addition to the exterior aqueous phase. Intraliposome $[Ca^{2+}]$ increased from 300 to

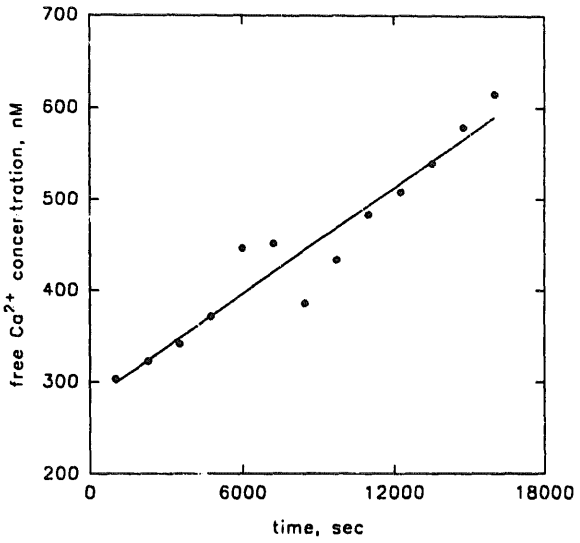

Fig. 1. Typical intraliposome free calcium ion concentration ($[Ca^{2+}]_i$; nM) as a function of time (s) under static, zero shear conditions. $[Ca^{2+}]_i$ is estimated from fluorescence of intraliposome indo-1^{5-}. Fluorescence measurement was halted after 14400 s, before Ca^{2+} saturation of the indo-1^{5-} (approx. 2000 nM). Data points are shown with the best-fit linear approximation.

650 nM during 5 h of static exposure to physiological extraliposomal free calcium ion concentration ($[Ca^{2+}]_o$). The $[Ca^{2+}]_o$, initially fixed at 1 mM, remained essentially constant during the experiment. The Ca^{2+} concentration difference across the membrane (δC) also remained essentially constant throughout the experiment (at $t = 0$, $\Delta C = 9.9965 \cdot 10^{+5}$ nM; at $t = 5$ h, $\Delta C = 9.993 \cdot 10^{+5}$ nM (as calculated from a Ca^{2+} balance)). Total liposome volume (V) and total surface area (SA) also remain constant during the experiment (Fig. 6). Under these conditions, the increase in $[Ca^{2+}]_i$ is expected to be a linear function of time with constant slope. The calculated trans-bilayer Ca^{2+} flux is also constant.

A control experiment was carried out to estimate the degree of indo-1^{5-} leakage through the liposome membrane. A sample of freshly prepared liposomes containing indo-1^{5-} was divided into two aliquots. Fluorescence response to the addition of 1 mM $[Ca^{2+}]_o$ was measured shortly after liposome preparation in the first aliquot. The concentration of extraliposome indo-1^{5-} is reflected by a step change in fluorescence immediately after Ca^{2+} addition. The second, identical aliquot was maintained at room temperature without addition of Ca^{2+} to the exterior aqueous phase. After 5 h, the $[Ca^{2+}]_o$ in the second aliquot was raised to 1 mM and the change in fluorescence ratio was measured. The step increase in fluorescence intensity from baseline upon the addition of Ca^{2+} to the exterior aqueous phase was 7% greater in the stored aliquot than that measured immediately after liposome preparation.

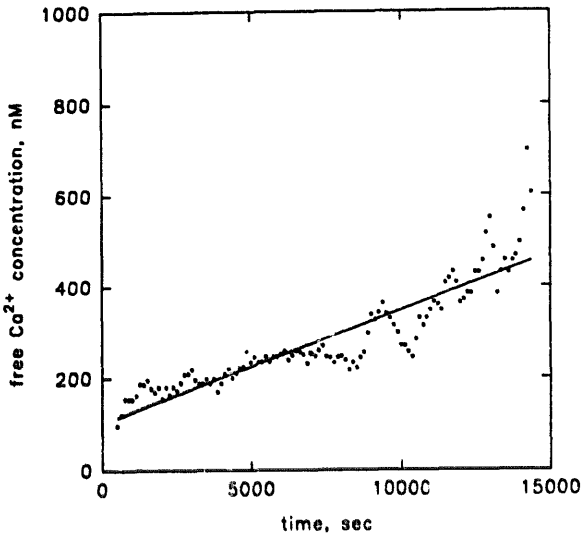

Fig. 2. Typical intraliposome free calcium ion concentration ($[Ca^{2+}]_i$; nM) as a function of time (s) during exposure to a uniform, controlled shear rate of 27 s^{-1}. $[Ca^{2+}]_i$ is estimated from fluorescence of intraliposome indo-1^5. Fluorescence measurement was halted after 14400 s, before Ca^{2+} saturation of the indo-1^5 (approx. 2000 nM). Data points are shown with the best-fit linear approximation.

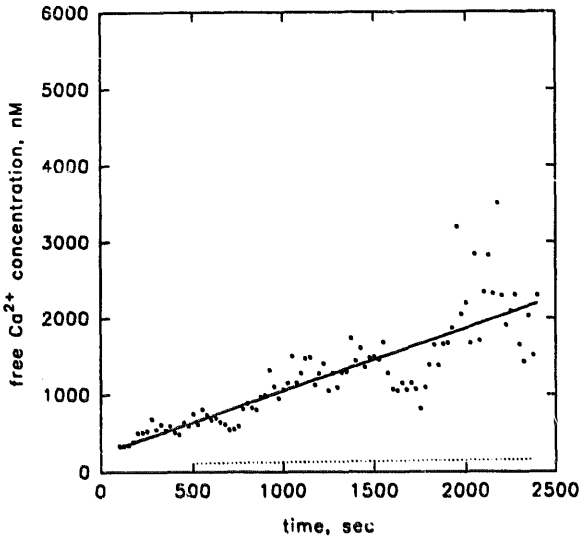

Fig. 3. Typical intraliposome free calcium ion concentration ($[Ca^{2+}]_i$; nM) as a function of time (s) during exposure to a uniform, controlled shear rate of 1350 s^{-1}. $[Ca^{2+}]_i$ is estimated from fluorescence of intraliposome indo-1^5. Fluorescence measurement was halted near Ca^{2+} saturation of the indo-1^5 (approx. 2000 nM). Data points are shown with the best-fit linear approximation. The dashed line represents $[Ca^{2+}]_i$ at 27 s^{-1} (from Fig. 2) shown for comparison.

The effect of indo-1^5 photobleaching, studied by continuous fluorescence measurement of Hepes-buffered saline containing 1 μM indo-1^5 and 1 mM Ca^{2+} for 5 h, was not significant.

Calcium transport across liposome membranes exposed to uniform shear stress

Dynamic studies of liposome permeability to Ca^{2+} were performed during application of uniform, controlled fluid shear at rates attained in the normal mammalian cardiovasculature (2700, 1350, and 27 s^{-1}). Duplicate experiments were performed with each of two independently prepared liposome samples.

Intraliposome free $[Ca^{2+}]$ is shown as a function of shear exposure time in Figs. 2–4 for each of three different applied fluid shear intensities. Shear stress exposure was terminated at 14400 s ($\dot{\gamma} = 27$ s^{-1}) or when $[Ca^{2+}]_i$ reached approx. 2 μM (2400 s for $\dot{\gamma} =$ 1350 s^{-1}; 840 s for $\dot{\gamma} = 2700$ s^{-1}). Data shown in Figs. 2–4 is representative of all experiments conducted (Table I). Indo-1^5 fluorescence is relatively insensitive to free $[Ca^{2+}]$ above 2 μM as complete Ca^{2+}-indo-1^5 chelation is approached. Initial $[Ca^{2+}]_i$ ranged from 95 to 400 nM and reflects a low level of Ca^{2+} contamination from environmental and reagent sources. Intraliposome $[Ca^{2+}]$ increased with time in response to all levels of applied fluid stress. The rate of $[Ca^{2+}]_i$ rise increased as a function of applied shear rate. Differences in liposome permeability as a function of applied fluid stress were statistically significant (Table I).

The calculated trans-bilayer Ca^{2+} flux was normalized by the flux estimated under static conditions. This presentation highlights the percentage increase in trans-bilayer Ca^{2+} flux as a function of applied fluid force. The normalized flux increased linearly with the shear rate (Fig. 5, Table I). The slope of the normalized Ca^{2+} flux versus shear rate line was significantly different from zero (ANCOVA, $P < 0.01$).

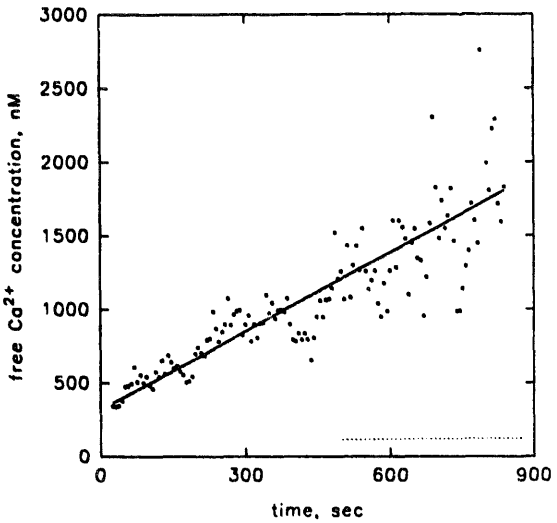

Fig. 4. Typical intraliposome free calcium ion concentration ($[Ca^{2+}]_i$; nM) as a function of time (s) during exposure to a uniform, controlled shear rate of 2700 s^{-1}. $[Ca^{2+}]_i$ is estimated from fluorescence of intraliposome indo-1^5. Fluorescence measurement was halted near Ca^{2+} saturation of the indo-1^5 (approx. 2000 nM). Data points are shown with the best-fit linear approximation. The dashed line represents $[Ca^{2+}]_i$ at 27 s^{-1} (from Fig. 2) shown for comparison.

TABLE I

Fluid force effect on egg PC bilayer Ca^{2+} flux

Net trans-bilayer calcium ion flux (nmol/cm^2 per s) is shown as a function of applied shear rate (s^{-1}). Results are averaged from four independent experiments conducted at each shear rate. The calcium ion flux at each shear rate is also shown normalized with the calcium ion flux under static, no flow conditions. This presentation highlights the influence of fluid force on egg PC bilayer permeability. All Ca^{2+} flux values determined at different shear rates are significantly different ($P < 0.001$, Student's t-test of means) except static vs. 27 s^{-1} ($P < 0.10$, Student's t-test of means).

Shear rate (s^{-1})	Ca^{2+} flux (nmol/cm^2 per s)	Standard deviation (nmol/cm^2 per s)	Normalized Ca^{2+} flux
static	$4.7 \cdot 10^{-10}$	$\pm 6.4 \cdot 10^{-11}$	1
27	$5.8 \cdot 10^{-10}$	$\pm 7.7 \cdot 10^{-11}$	1.3
1350	$2.0 \cdot 10^{-8}$	$\pm 2.2 \cdot 10^{-10}$	42
2700	$4.4 \cdot 10^{-8}$	$\pm 8.5 \cdot 10^{-10}$	94

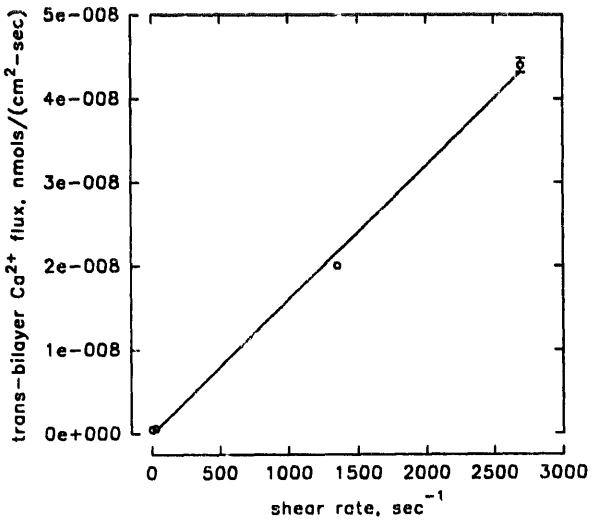

Fig. 5. Net trans-bilayer calcium ion flux (nmol/cm^2 per s) is shown as a function of applied shear rate (s^{-1}). Data points are averaged from four independent experiments conducted at each shear rate. Error bars represent ± one standard deviation. The best-fit linear approximation shown has a slope of $1.6 \cdot 10^{-11}$ (nmol/cm^2), which is significantly different from zero (ANCOVA, $P < 0.01$).

TABLE II

Lipsome size statistics before and after exposure to shear stress

The total count indicates the number of particles counted per 100 μl of suspension. Average particle diameter, surface area and volume are calculated from the entire particle diameter distribution measured from 0.5 μm to 10 μm. Results are shown as mean ± S.D.; $n = 7$. No parameter was significantly altered as a result of shear exposure (paired t-test, $P > 0.2$).

	Before shear	After shear
Total count	$(1.58 \pm 0.46) \cdot 10^5$	$(1.54 \pm 0.31) \cdot 10^5$
Particle diameter (μm)	1.06 ± 0.05	1.05 ± 0.05
Particle surface area (μm^2)	3.52 ± 0.32	3.49 ± 0.35
Particle volume (μm^3)	0.81 ± 0.09	0.79 ± 0.10

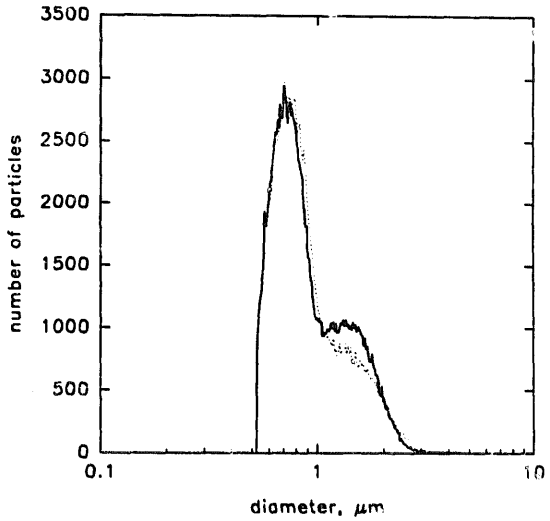

Fig. 6. Typical liposome size distribution shown before (———) and after (· · · · · ·) exposure to uniform, controlled fluid shear (1350 s^{-1}). Total surface area for this sample was $5.80 \cdot 10^{+5}/5.81 \cdot 10^{+5}$ (before shear/after shear; μm^2); total liposome volume for this sample was $1.37 \cdot 10^{+5}/1.39 \cdot 10^{+5}$ (before shear/after shear; μm^3).

Liposome size distribution was not significantly changed as a result of exposure to any shear stress duration or intensity studied (Fig. 6). The number of relatively large particles, presumed to be liposome aggregates, appeared to be reduced after shear exposure. Liposome diameter, surface area and volume were not altered by fluid shear exposure (Table II).

Discussion

Liposomes prepared as described here were macroscopically stable to application of fluid stress. Particle size distribution, total liposome surface area and total entrapped volume were not significantly altered as a result of fluid shear exposure. The extrusion technique prepares stable liposomes [22] with a very narrow size distribution centered near the membrane pore diameter [19,20]. Particles with diameters larger than approx. 1 μm are presumed to be small liposome aggregates coordinated through ionic interactions [23,24]. The presence of aggregates formed by liposome fusion can not be ruled out. Liposome fusion in similar systems, however, occurs without leakage of the entrapped volume [25]. The slight reduction in number of these larger particles after shear exposure is presumed to result from temporary disaggregation induced by shear force exposure. Macroscopic physical liposome disruption is not supported by an order of magnitude force estimate (described below) which suggests that the liposome area increase induced by shear stress is much less than the critical liposome area increase required for vesicle failure ($\alpha \ll \alpha_c$).

A small fraction of the unencapsulated indo-1^{5-} remained in the external aqueous phase after gel filtra-

tion. Elution profiles of liposomes and unencapsulated indo-1^{5-} from the gel filtration column were well separated. Indo-1^{5-} available in the outer aqueous phase is presumed to be associated with the outer bilayer surface. Indo-1^{5-} leakage is estimated to be 7% per 5 h, a rate insufficient to influence the estimates of intraliposome $[Ca^{2+}]$. Changes in 410 nm/490 nm fluorescence ratio were presumed to be due to Ca^{2+} influx rather than indo-1^{5-} efflux.

In the absence of changing free $[Ca^{2+}]_i$, continuous illumination altered the sample fluorescence ratio by less than 3% over a period of 5 h. The lack of observable photobleaching is attributed to the small volume fraction (0.17%) of the continuously illuminated sample.

Calcium ion trans-bilayer flux measured by this technique in the absence of fluid shear ($4.7 \cdot 10^{-10}$ nmol/cm^2 per s) is comparable to other published results [15,16,26,27] in similar systems. Water [5–7], hydrogen ion [6,7] and sodium ion [5] permeate lipid bilayers more easily than does calcium ion. Lipid composition and geometry also influence experimentally measured bilayer permeability [5–7].

Net trans-bilayer Ca^{2+} flux is a strong function of applied fluid shear. The total mass transfer resistance across a liposome is the sum of diffusive resistance of the lipid bilayer and the convective resistance of the fluid film as given by:

$$\frac{J_a}{A} = \frac{(C_{a,o} - C_{a,i})}{\frac{\delta}{D_m} + \frac{1}{k_i} + \frac{1}{k_o}}$$

where J_a is the trans-bilayer Ca^{2+} flux (nmol/s), A is the total liposome surface area (cm^2), $C_{a,i}$ is the free $[Ca^{2+}]$ inside the liposome (nmol/cm^3), $C_{a,o}$ is the free $[Ca^{2+}]$ outside the liposome (nmol/cm^3), δ is the liposome membrane thickness (cm), D_m is the diffusive resistance of the membrane (or membrane permeability^{-1}) (cm^2/s), $1/k_i$ is the convective resistance of the inner fluid film (s/cm) and $1/k_o$ is the convective resistance of the outer fluid film (s/cm).

Inner convective resistance of the small liposome interior can be neglected compared to the outer convective resistance. The total convective mass transfer resistance ($1/k_t$) is then the sum of the membrane diffusional resistance and the outer convective resistance:

$$\frac{1}{k_t} = \frac{\delta}{D_m} + \frac{1}{k_o}$$

Correlations for flow around rigid spheres may be used to estimate the outer convective mass transfer resistance [28,29]. The relative fluid-particle velocity is somewhat ambiguous and difficult to estimate. The maximum outer convective resistance occurs as the fluid velocity approaches zero. Assumption of zero fluid velocity difference is valid for small, neutrally buoyant particles travelling at approximately the same velocity as the local fluid velocity. The Sherwood number for mass transfer ($N_{Sh,m}$) asymptotically approaches two as the fluid velocity difference approaches zero. Both the outer convective mass transfer coefficient (k_o, calculated from correlations) and the total mass transfer coefficient (k_t, calculated from the experimentally determined trans-bilayer Ca^{2+} flux) increase with applied shear rate (Fig. 7). The total mass transfer coefficient, however, is at least 10 orders of magnitude smaller than the outer convective mass transfer coefficient at all shear rates. Trans-bilayer Ca^{2+} transport in liposomes is diffusion limited at the lipid bilayer in static and dynamic fluid environments. Overall mass transfer resistance across the liposome membrane is essentially equal to the diffusional resistance of the lipid bilayer

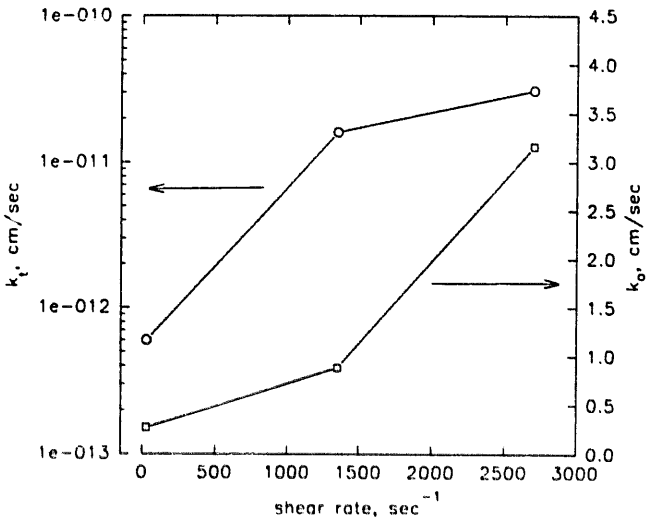

Fig. 7. Outer convective mass transfer coefficient (k_o, □) and total mass transfer coefficient (k_t, ○) for passive Ca^{2+} trans-bilayer transport as a function of applied shear rate. k_o is estimated from numerical correlations for mass transfer from a submerged sphere; k_t is calculated from the experimentally obtained trans-bilayer Ca^{2+} flux.

$$\frac{1}{k_t} \approx \frac{\delta}{D_m}$$

Thus, decreasing overall mass transfer resistance (as a function of applied fluid shear) is due to decreasing liposome bilayer permeability. Modification of bilayer permeability though application of physical force has been demonstrated in other liposome systems [10,11]. Fluid stress-induced modification of lipid bilayer structure is presumed to be responsible for increased liposome permeability during fluid shear exposure. Fluid force application may directly influence the molecular area (A_M) of the bilayer and increase the number of

bilayer packing defects through which passive Ca^{2+} transport is believed to occur.

Careful studies of bilayer compressibility in cells [30] and liposomes [31] have been carried out using a micropipette technique. Application of a controlled pressure differential imposes a force which produces a uniform surface tension in the partially aspirated liposome or cell. Lipid bilayer compressibility (K_a) may be estimated from measurement of the uniform surface tension ($\bar{T}$) and the fractional change in membrane area (α)

$$\bar{T} = K_a \cdot \alpha$$

This study does not propose to determine bilayer compressibilities. Fluid forces developed in the cone and plate rotational viscometer are well characterized, but the force distribution on a particle exposed to shear varies with the particle surface curvature. A pure shear force, for example, acts normal to the surface at the leading and trailing portions of liposome. The same force acts tangent to bilayer surface 90° from the leading and trailing edges. Restated simply, the shear force vectors act in different relative orientations along the curved liposome surface. Calculation of the shear force distribution on a suspended liposome is beyond the scope of this work. In addition, rotational viscometers develop elongational forces at high shear rates which may play a significant role in bilayer deformation [32,33].

If the shear force were assumed to induce a uniform surface tension, published values of K_a may be used to estimate the fractional change in membrane area (α). A stress of 33.3 dyne/cm^2 would produce a uniform tension of $33.3 \cdot 10^{-6}$ dyne/cm in a lipid bilayer of thickness $1 \cdot 10^{-6}$ cm [34]. For a phosphatidylcholine bilayer compressibility of 193 dyne/cm [31], the resulting fractional change in membrane area is $173 \cdot 10^{-9}$. The critical fractional membrane area increase before failure in a phosphatidylcholine liposome is $30 \cdot 10^{-3}$ [31]. Because the force is not distributed uniformly, some portions of the liposome will experience surface tension greater than the average assumed in this estimate with correspondingly greater local fractional membrane area change. The actual average change in membrane area is, however, less than predicted from this calculation because some of the shear force does not contribute to membrane tension.

Fluid force-induced changes in lipid bilayer permeability are of potential significance in cardiovascular applications of liposome techniques. The shear rates applied in this study (27 to 2700 s^{-1}) are observed in the human cardiovasculature. This study suggests that, at least for small solutes such as Ca^{2+}, fluid shear such as obtained in the human cardiovasculature induces an increase in liposome permeability of up to two orders of magnitude. Additional studies are underway to investigate the influence of solute parameters and liposome properties (such as size and composition) on the magnitude of fluid shear enhanced liposome permeability. The relationship between bilayer compressibility and liposome susceptibility to fluid stress-induced permeability changes is also under study.

The influence of fluid forces on liposome permeability is of potential significance in the pharmacokinetics of injectable liposome applications. Increased permeability of liposomes in shear fields, such as demonstrated in this study, may be utilized to release encapsulated material preferentially in regions of elevated fluid shear. The translation of liposome performance data from non-flow, cell culture studies to flowing systems (such as the mammalian cardiovasculature) must include consideration of fluid stress-induced changes in bilayer permeability.

Acknowledgements

This study was supported by a Whitaker Foundation award. Additional support was provided by the Vanderbilt University Research Council.

References

1 Francis, S.E., Lyle, I.G. and Jones, M.N. (1991) Biochim. Biophys. Acta 1062, 117–122.
2 Isaacson, Y., Riehl, T.E. and Stenson, W.F. (1989) Biochim. Biophys. Acta 986, 295–300.
3 Kurantsin-Mills, J. and Boggs, J.M. (1986) Biotech. Appl. Biochem. 8, 69–74.
4 Malinski, J.A. and Nelsestuen, G.L. (1989) Biochemistry 28, 61–70.
5 Cruzeiro-Hansson, L. and Mouritsen, O.G. (1988) Biochim. Biophys. Acta 944, 63–72.
6 Deamer, D.W. and Bramhall, J. (1986) Chem. Phys. Lipids 40, 167–188.
7 Garlid, K.D., Beavis, A.D. and Ratkje, S.K. (1989) Biochim. Biophys. Acta 976, 109–120.
8 Barchfeld, G.L. and Deamer, D.W. (1988) Biochim. Biophys. Acta 944, 40–48.
9 Kjaer, K., Als-Nielsen, J., Helm, C.A., Laxhuber, L.A. and Möhwald, H. (1987) Phys. Lett. Rev. 58, 2224–2227.
10 Needham, D. and Hochmuth, R.M. (1989) Biophys. J. 55, 1001–1009.
11 Saalman, E., Norden, B., Arvidsson, L., Hamnerius, Y., Hojevik, P., Connell, K.E. and Kurucsev, T. (1991) Biochim. Biophys. Acta 1064, 124–130.
12 Parsegian, V.A., Fuller, N.L. and Rand, R.P. (1979) Proc. Natl. Acad. Sci. USA 76, 2750–2754.
13 Rand, R.P. (1981) Annu. Rev. Biophys. Bioeng. 10, 277–314.
14 Nagle, J.F. and Scott, H.L. (1978) Biochim. Biophys. Acta 513, 236–243.
15 Blau, L. and Weissman, G. (1988) Biochemistry 27, 5661–5666.
16 Utsumi, K., Nobori, K., Terada, S., Miyahara, M. and Utsumi, T. (1985) Cell Struct. Funct. 10, 339–348.
17 Roe, J.N., Szoka, F.C. and Verkman, A.S. (1989) Biophys. Chem. 33, 295–302.

18 Verkman, A.S., Takla, R., Sefton, B., Basbaum, C. and Widdicombe, J.H. (1989) Biochemistry 28, 4240–4244.
19 Hope, M.J., Bally, M.B., Webb, G. and Cullis, P.R. (1985) Biochim. Biophys. Acta 812, 55–65.
20 Mayer, L.D., Hope, M.J. and Cullis, P.R. (1986) Biochim. Biophys. Acta 858, 161–168.
21 Grynkiewicz, G., Poenie, M. and Tsein, R.Y. (1985) J. Biol. Chem. 260, 3440–3450.
22 Lesieur, S., Grabielle-Madelmont, C., Paternostre, M.T. and Ollivon, M. (1991) Anal. Biochem. 192, 334–343.
23 Bentz, J., Düzgüneş, N. and Nir, S. (1985) Biochemistry 24, 1064–1072.
24 Eklund, K.K., Takkunen, J.E. and Kinnunen, P.K. (1991) Chem. Phys. Lipids 57, 59–66.
25 Wilschut, J., Düzgüneş, N., Fraley, R. and Papahadjopoulos, D. (1980) Biochemistry 19, 6011–6021.
26 Erdreich, A. and Rahamimoff, H. (1987) Biochem. Pharmacol. 36, 1775–1780.
27 Holmes, R.P., Mahfouz, M., Travis, B.D., Yoss, N.L. and Keenan, M.J. (1983) Ann. of the N.Y. Acad. Sci. 414, 44–55.
28 Ranz, R.E. and Marshall, W.R.J. (1952) Chem. Eng. Prog. 48, 141–146.
29 Ranz, R.E. and Marshall, W.R.J. (1952) Chem. Eng. Prog. 48, 173–180.
30 Evans, E.A., Waugh, R. and Melnik, L. (1976) Biophys. J. 16, 585–595.
31 Needham, D. and Nunn, R.S. (1990) Biophys. J. 58, 997–1009.
32 Fewell, M.E. and Hellums, J.D. (1977) Trans. Soc. Rheol. 21, 535–565.
33 Purvis, J., NB and Giorgio, T.D. (1991) Biorheology 28, 355–367.
34 Evans, E.A. and Hochmuth, R.M. (1978) Curr. Top. Membr. Transp. 10, 1–64.